

考虑渗流效应的深埋海底隧道围岩与衬砌结构应力场研究

金波, 胡明, 方棋洪

RESEARCH ON STRESS FIELD OF SURROUNDING ROCK AND LINING STRUCTURE OF DEEP-BURIED SUBSEA TUNNEL CONSIDERING SEEPAGE EFFECT

Jin Bo, Hu Ming, and Fang Qihong

在线阅读 View online: <https://doi.org/10.6052/0459-1879-21-670>

您可能感兴趣的其他文章

Articles you may be interested in

微磁检测应力和塑性区的磁弹塑耦合理论

THEORETICAL MODEL OF MAGNETO-ELASTOPLASTIC COUPLING FOR MICRO-MAGNETIC NON-DESTRUCTIVE TESTING METHOD WITH STRESS CONCENTRATION AND PLASTIC ZONE

力学学报. 2021, 53(12): 3341-3353

多个椭圆柱波浪力的一种解析解

AN ANALYTICAL SOLUTION FOR WAVE PRESSURE ON ARRAYS OF ELLIPTICAL BODIES

力学学报. 2021, 53(11): 3157-3167

基于XFEM-MBEM的嵌入式离散裂缝模型流固耦合数值模拟方法

NUMERICAL SIMULATION FOR COUPLING FLOW AND GEOMECHANICS IN EMBEDDED DISCRETE FRACTURE MODEL BASED ON XFEM-MBEM

力学学报. 2021, 53(12): 3413-3424

三剪应力统一强度理论研究

STUDY OF THREE-SHEAR STRESS UNIFIED STRENGTH THEORY

力学学报. 2017, 49(6): 1322-1334

金属/环氧/金属粘结体系的强韧和失效机制实验研究

EXPERIMENTAL INVESTIGATIONS OF STRENGTH, TOUGHNESS AND FAILURE MECHANISM OF THE METAL/EPOXY/METAL ADHESIVE SYSTEM

力学学报. 2017, 49(6): 1213-1222

低密度风洞瑞利散射测速实验中纳米粒子跟随性数值分析

NUMERICAL ANALYZITION OF NANO-PARTICLE FOLLOWING FEATURES FOR RAYLEIGH SCATTERING VELOCITY MEASUREMENT TEST IN LOW DENSITY WIND TUNNEL

力学学报. 2017, 49(6): 1243-1251



考虑渗流效应的深埋海底隧道围岩与衬砌结构 应力场研究¹⁾

金 波^{*,†,2)} 胡 明^{*} 方棋洪^{**}

^{*} (湖南大学土木工程学院, 工程结构损伤诊断湖南省重点实验室, 长沙 410082)

[†] (湖南湖大建设监理有限公司, 长沙 410082)

^{**} (湖南大学机械与运载工程学院, 长沙 410082)

摘要 深埋海底隧道经常处于高压工况, 地下水渗流对隧道围岩及衬砌结构安全性有较大影响. 本文提出了一种含衬砌深埋海底隧道力学模型, 研究了海底隧道服役阶段地下水渗流对围岩及衬砌结构稳定性的影响机理. 应用保角映射方法将包含海水与围岩弹性区的半无限域映射成圆环域, 根据渗流边界条件建立了各界面间极坐标下的渗流方程, 得到了海底隧道渗流场解析解. 将渗流场以体积力形式作用到应力场中, 根据应力边界条件建立了应力平衡方程, 基于考虑中间主应力影响的 Drucker-Prager (D-P) 准则, 得到了渗流效应影响下围岩与衬砌结构的弹塑性解析解. 以深圳妈湾跨海通道工程为例, 将解析解与有限元数值解进行了对比, 验证了本文理论解的准确性, 研究了渗流效应对隧道围岩与衬砌结构应力场的影响规律. 最后, 分析了海水深度与内水水头对塑性区半径的影响. 研究表明: 渗流效应对围岩与衬砌结构中的环向应力影响显著, 径向应力随 ρ 增大呈非线性增长; 随着海水加深, 隧道承受水压不断加大, 围岩塑性区范围显著增大; 增加内水水头可以有效限制围岩塑性区发展, 初始阶段限制效果明显, 后续增加内水水头限制效果逐渐减弱.

关键词 深埋海底隧道, 渗流效应, 保角映射, Drucker-Prager 准则, 弹塑性解析解

中图分类号: U451 文献标识码: A doi: 10.6052/0459-1879-21-670

RESEARCH ON STRESS FIELD OF SURROUNDING ROCK AND LINING STRUCTURE OF DEEP-BURIED SUBSEA TUNNEL CONSIDERING SEEPAGE EFFECT¹⁾

Jin Bo^{*,†,2)} Hu Ming^{*} Fang Qihong^{**}

^{*} (Key Laboratory for Damage Diagnosis of Engineering Structures of Hunan Province, College of Civil Engineering, Hunan University, Changsha 410082, China)

[†] (Hunan Huda Construction Supervision Co., Ltd., Changsha 410082, China)

^{**} (College of Mechanical and Vehicle Engineering, Hunan University, Changsha 410082, China)

Abstract Deep-buried subsea tunnels are often under high water pressure condition and therefore groundwater seepage exerts a great impact on the surrounding rock and lining structure safety. In this paper, a mechanical model of deep-buried subsea tunnel with lining is proposed to study the influence mechanism of groundwater seepage on the surrounding rock and lining structure stability during the service stage of subsea tunnel. Firstly, a conformal mapping

2021-12-16 收稿, 2022-03-18 录用, 2022-03-19 网络版发表.

1) 国家自然科学基金资助项目 (11772122).

2) 金波, 副教授, 主要研究方向: 结构优化设计、工程结构力学. E-mail: jinbo@hnu.edu.cn

引用格式: 金波, 胡明, 方棋洪. 考虑渗流效应的深埋海底隧道围岩与衬砌结构应力场研究. 力学学报, 2022, 54(5): 1322-1330

Jin Bo, Hu Ming, Fang Qihong. Research on stress field of surrounding rock and lining structure of deep-buried subsea tunnel considering seepage effect. *Chinese Journal of Theoretical and Applied Mechanics*, 2022, 54(5): 1322-1330

method is adopted to map the semi-infinite domain which includes seawater and surrounding rock elastic zone into an annular domain, and the seepage equation in polar coordinates between interfaces is established according to the seepage boundary conditions. Thus, the analytical solution of the seepage field of the subsea tunnel is obtained. Secondly, the seepage field is applied to the stress field in the form of volume force, the stress balance equation is established according to the stress boundary conditions, and based on the Drucker-Prager (D-P) criterion which takes account of the effect of the intermediate principal stress, an elastoplastic analytical solution is derived for the surrounding rock and lining structure under the influence of seepage effect. Finally, taking Shenzhen Mawan Sea-Crossing Passage as an engineering example, the analytical solution is compared with the finite element numerical solution, which verifies the accuracy of the theoretical solution in this paper, the influence law of seepage effect on the stress field of tunnel surrounding rock and lining structure is studied, and the factors influencing the radius of surrounding rock plastic zone are analyzed. The results show that: the seepage effect has a significant influence on the hoop stress in surrounding rock and lining structure, and the radial stress increases nonlinearly with the increase of ρ . As the seawater goes deeper, the water pressure on tunnel continues to increase, and the surrounding rock plastic zone increases significantly. An increase in the internal water head can effectively limit the development of the surrounding rock plastic zone, with the initial limiting effect being obvious while the subsequent effect being gradually weakened.

Key words deep-buried subsea tunnel, seepage effect, conformal mapping, Drucker-Prager criterion, elastoplastic analytical solution

引言

随着我国经济飞速发展和综合国力不断提升, 跨海交通的需求与日俱增. 海底隧道因其独特的优势, 逐渐在现代交通工程中发挥重要作用^[1-3]. 近年来, 我国已建成和在建海底隧道数量日益增多, 如厦门翔安海底隧道、青岛胶州湾海底隧道、深圳妈湾跨海通道^[4-5]等, 同时, 多条长大跨海隧道正在筹划建设中, 如台湾海峡隧道、烟大渤海海峡隧道、琼州海峡隧道等^[6]. 可以预见, 在未来一段时间内我国海底隧道建设将进入飞速发展阶段.

海底隧道深埋于海底, 在其开挖周围水源丰富, 地下水渗流对隧道围岩及衬砌结构应力场和位移场的影响不可忽视, 尤其在高压水况下, 渗流效应导致围岩塑性损伤区持续扩大, 从而改变围岩及衬砌结构的应力状态和形变, 严重影响隧道的稳定性和安全性^[7-9]. 因此, 对渗流效应影响下深埋的海底隧道应力与形变的研究具有重要的理论意义和工程价值.

近年来, 国内外学者针对隧道围岩应力场和位移场问题进行了研究, 主要是通过弹塑性本构关系进行理论解析^[10-17]和数值模拟^[18-20].

在理论解析方面, 基于均匀地应力假设, Lee 和 Pietruszczak^[10]分别选取 Mohr-Coulomb (M-C) 准则和 Hoek-Brown (H-B) 准则作为围岩本构模型, 并采用一种简化的数值方法计算了考虑围岩应变软化效应的圆形洞室应力场和位移场; Li 等^[11]考虑渗流效

应和应力释放影响, 推导了深埋圆形隧洞的弹塑性解; Li 等^[12]基于统一强度理论, 推导了考虑渗流效应和地应力影响的深埋圆形隧道统一解; 邹金峰等^[13]基于 M-C 准则与应力-应变软化模型, 推导出圆形隧道软化围岩应力-应变的解析解, 该解考虑了轴向力与渗透力的影响; 在数值模拟方面, Hu 等^[18]采用有限元方法对双线重叠隧道的变形响应进行了研究, 证明隧道截面形式对双线重叠隧道的形变影响显著; Mu 等^[19]建立了一种软岩隧道长期变形破坏的计算模型, 进一步研究了软岩隧道的损伤演化过程及失稳破坏特性.

有关围岩-衬砌体系稳定性问题的研究也有诸多成果^[21-30]. 何川等^[21]基于 Drucker-Prager (D-P) 屈服准则, 研究了渗流效应影响下盾构隧道围岩与衬砌结构的相互作用; 张顶立等^[22]研究了支护结构体系与围岩的协同作用关系; Ma 等^[23]针对弹塑性界面存在于围岩中的情况, 基于线性 M-C 屈服准则, 推导出含衬砌圆形受压隧道的弹塑性解答.

目前, 针对隧道围岩应力场及围岩-衬砌体系稳定性的问题已进行了深入研究, 但是综合考虑渗流效应与围岩-衬砌体系稳定性的深埋海底隧道研究较少. 此外, 以往学者在进行渗流效应影响下深埋隧道力学特性研究时, 大都基于 M-C 准则对隧道围岩进行弹塑性分析, 但该准则忽略了中间主应力的影响, 对围岩屈服或破坏的解释相比实际情况存在较大偏差^[21].

为了使此类问题的求解结果更加符合实际工程, 本文建立了由海水、岩体及衬砌结构组成的海底隧道力学模型, 基于保角映射方法和考虑中间主应力影响的 D-P 准则, 推导了隧道围岩渗流场及渗流效应影响下围岩与衬砌结构的应力场, 研究了渗流效应对隧道围岩与衬砌结构应力场的影响规律, 分析了海水深度、内水水头对围岩塑性区半径的影响, 以期对深海隧道的设计与施工提供理论参考.

1 力学模型

为了适当简化研究问题, 本文基于以下假设^[7-13]: (1) 隧道位于连续均质、各向同性岩体中, 受均匀地应力作用, 水和海底岩体都不可压缩; (2) 隧道围岩中具有稳定渗流场, 且水源补给充足; (3) 渗流满足达西定律和质量守恒定律; (4) 隧道开挖后围岩自身稳定, 不会发生坍塌; (5) 围岩为弹塑性介质, 衬砌结构为线弹性材料.

根据基本假定, 建立了海底圆形衬砌式隧道力学模型, 如图 1 所示. 将通过隧道中心的虚线设为零位势线. 地应力 P_0 , 衬砌结构内侧压力 P_a , 海床位于海平面以下 d_1 , 隧道在海底岩体中开挖半径 r_l , 海平面和海床到隧道中心距离分别为 h_0 和 d_2 , 且 $h_0 = d_1 + d_2$. 围岩-衬砌界面和围岩弹塑性区界面的法向接触压力分别为 p_l 和 p_p , h_l 和 h_p 分别为两界面的渗流水头. 内水水头为 h_a , 围岩塑性区到海床距离为 h . 设 ρ 为隧道洞室中心沿径向向外的距离. 设 Q_0 为通过隧道外侧圆环断面的地下水渗流量. 隧道衬砌结构内半

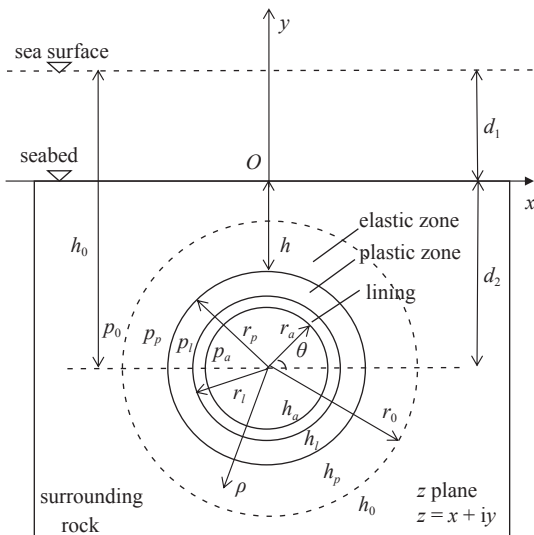


图 1 海底衬砌隧道力学模型

Fig. 1 Mechanical model of subsea lining tunnel

径 r_a , 其材料渗透系数 k_l ; 围岩塑性区半径 r_p , 其渗透系数 k_p ; 围岩塑性区以外定义为弹性介质, 围岩弹性区半径 $r_0 = \lambda r_a \rightarrow \infty$, 根据工程实际和安全性要求, λ 取为 20 即可满足相关要求^[11], 其渗透系数 k_r . 此外, 围岩塑性区与衬砌结构在图 1 力学模型中均为圆环, 因此采用极坐标求解更为简便.

2 渗流场解析解

2.1 围岩弹性区渗流场

应用保角映射方法, 将围岩塑性区外边界、海底岩体和海平面映射成一个圆环, 如图 2 所示, 映射函数为^[31]

$$z = \omega(\xi) = iA \frac{1 + \xi}{1 - \xi} \tag{1a}$$

或

$$\xi = f(z) = \frac{z + iA}{z - iA} \tag{1b}$$

式中

$$A = \frac{h(1 - \alpha^2)}{1 + \alpha^2} = \sqrt{h^2 - r_p^2}$$

$$\alpha = \frac{h}{r_p} - \sqrt{\left(\frac{h}{r_p}\right)^2 - 1}$$

将 Z 平面上的任意点 (x, y) 用 (ρ, θ) 共形映射到 ξ 平面上.

根据达西定律和质量守恒定律, 可得围岩 (轴对称) 中渗流方程的极坐标表达式

$$\frac{\partial^2 \phi_r}{\partial \xi^2} + \frac{\partial^2 \phi_r}{\partial \eta^2} = 0 \tag{2}$$

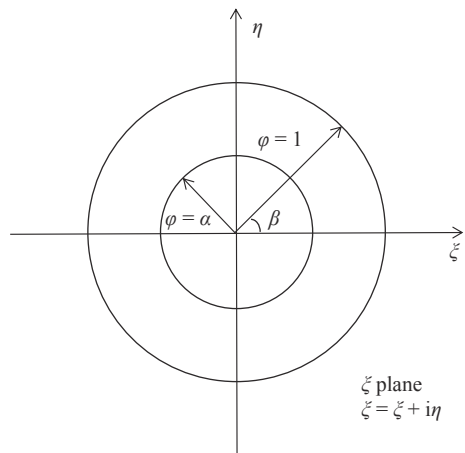


图 2 保角映射区域

Fig. 2 Conformal mapping area

式中, ϕ_r 为围岩中压力总水头。

在 ξ 平面内, 式 (2) 的通解可采用级数形式表示^[32]

$$\phi = C_1 + C_2 \ln \varphi + \sum_{n=1}^{\infty} (C_3 \varphi^n + C_4 \varphi^{-n}) \cos(n\beta) \quad (3)$$

式中, C_1, C_2, C_3, C_4 为待定系数, 可由边界条件 $\phi_{(\varphi=1)} = h_0$ 和 $\phi_{(\varphi=\alpha)} = h_p$ 确定^[32]。

根据上述边界条件, 联立式 (2) 和式 (3), 可得围岩中压力总水头为

$$\phi_r = h_0 + \frac{\ln \varphi}{\ln \alpha} (h_p - h_0) \quad (4)$$

对式 (4) 进行积分, 可得围岩弹、塑性区界面的涌水量为

$$Q_r = k_r \int_0^{2\pi} \frac{\partial \phi_r}{\partial \varphi} \varphi d\beta = \frac{2\pi k_r}{\ln \alpha} (h_p - h_0) \quad (5)$$

2.2 围岩塑性区与衬砌结构渗流场

围岩塑性区与衬砌结构渗流微分方程形式相同, 可写为

$$\frac{\partial^2 \phi_{p,l}}{\partial \rho^2} + \frac{1}{\rho} \frac{\partial \phi_{p,l}}{\partial \rho} + \frac{1}{\rho^2} \frac{\partial \phi_{p,l}}{\partial \theta^2} = 0 \quad (6)$$

将围岩塑性区与衬砌结构中的渗流视为轴对称稳定渗流, 式 (6) 简写为

$$\frac{\partial^2 \phi_{p,l}}{\partial \rho^2} + \frac{1}{\rho} \frac{\partial \phi_{p,l}}{\partial \rho} = 0 \quad (7)$$

通过边界条件 $\phi_{l(\rho=r_a)} = h_a, \phi_{l(\rho=r_l)} = h_l, \phi_{p(\rho=r_l)} = h_l, \phi_{p(\rho=r_p)} = h_p$ 和 $\phi_{r(\rho=r_0)} = h_0$, 求解式 (7), 得

$$\left. \begin{aligned} \phi_p &= \frac{h_l \ln r_p - h_p \ln r_l}{\ln(r_p/r_l)} + \frac{h_p - h_l}{\ln(r_p/r_l)} \ln \rho \\ \phi_l &= \frac{h_a \ln r_l - h_l \ln r_a}{\ln(r_l/r_a)} + \frac{h_l - h_a}{\ln(r_l/r_a)} \ln \rho \end{aligned} \right\} \quad (8)$$

由式 (8) 可得围岩塑性区与衬砌结构界面及衬砌结构外侧的涌水量为

$$\left. \begin{aligned} Q_p &= \frac{2\pi k_p}{\ln(r_p/r_l)} (h_p - h_l) \\ Q_l &= \frac{2\pi k_l}{\ln(r_l/r_a)} (h_l - h_a) \end{aligned} \right\} \quad (9)$$

根据层间渗流连续相等原则, 即 $Q_0 = Q_r = Q_p = Q_l$, 联立式 (5) 和式 (9), 可得围岩塑性区与衬砌结构界面及衬砌结构外侧的渗流水头为

$$\left. \begin{aligned} h_p &= \frac{\frac{k_r}{k_p} h_0 \ln \left(\frac{r_p}{r_l} \right) - h_a \ln \left(\frac{d_2 + \sqrt{d_2^2 - r_p^2}}{r_p} \right)}{\ln \left(\frac{d_2 + \sqrt{d_2^2 - r_p^2}}{r_p} \right) + \frac{k_r}{k_p} \ln \left(\frac{r_p}{r_l} \right) + \frac{k_r}{k_l} \ln \left(\frac{r_l}{r_a} \right)} \\ h_l &= \frac{\frac{k_r}{k_l} h_0 \ln \left(\frac{r_l}{r_a} \right) - h_a \left[\frac{k_r}{k_p} \ln \left(\frac{r_p}{r_l} \right) + \ln \left(\frac{d_2 + \sqrt{d_2^2 - r_p^2}}{r_p} \right) \right]}{\ln \left(\frac{d_2 + \sqrt{d_2^2 - r_p^2}}{r_p} \right) + \frac{k_r}{k_p} \ln \left(\frac{r_p}{r_l} \right) + \frac{k_r}{k_l} \ln \left(\frac{r_l}{r_a} \right)} \end{aligned} \right\} \quad (10)$$

由 $P_{p,l} = \gamma_\omega (h_{p,l} - h_0)$ 可得围岩弹、塑性区界面及围岩与衬砌结构界面的压力。

3 渗流效应下的隧道应力场

实际施工过程中, 通常是待隧道围岩形变稳定后再进行衬砌。假设隧道开挖岩体弹性区弹性模量 E_e , 泊松比 μ_e ; 岩体塑性区弹性模量 E_p , 泊松比 μ_p , 黏聚力 c_p , 摩擦角 φ_p ; 衬砌结构弹性模量 E_l , 泊松比 μ_l 。

3.1 基本方程

基于平面应变假定, 模型各界面间存在内外水头差, 将由此产生的渗透力以体积力形式施加到隧道应力场中。围岩与衬砌结构中应力平衡方程为

$$\frac{d\sigma_\rho}{d\rho} + \frac{\sigma_\rho - \sigma_\theta}{\rho} + \gamma_\omega \frac{d(\xi H)}{d\rho} = 0 \quad (11)$$

式中, σ_ρ 为径向正应力, σ_θ 为环向正应力, 二者方向均以拉为正、压为负; γ_ω 为海水密度, ξ 为有效孔隙水压力系数。

3.2 衬砌结构应力场

衬砌结构中应力平衡方程为

$$\frac{d\sigma_\rho}{d\rho} + \frac{\sigma_\rho - \sigma_\theta}{\rho} + \frac{\gamma_\omega \xi (h_l - h_a)}{\rho \ln(r_l/r_a)} = 0 \quad (12)$$

边界条件

$$\left. \begin{aligned} (\sigma_\rho)_{\rho=r_a} &= -p_a \\ (\sigma_\rho)_{\rho=r_l} &= -p_l \end{aligned} \right\} \quad (13)$$

联立式 (12) 和式 (13), 基于弹性力学中求解平面应变问题的相关方法^[33], 得到衬砌结构中的应力场为

$$\left. \begin{aligned} \sigma_\rho^I &= \chi_1 + \chi_2 \rho^{-2} - \chi_3 \ln \rho \\ \sigma_\theta^I &= \chi_4 + \chi_2 \rho^{-2} - \chi_3 \ln \rho \end{aligned} \right\} \quad (14)$$

式中

$$\chi_1 = \frac{p_l r_l^2 - p_a r_a^2}{r_a^2 - r_l^2} + \frac{\gamma_\omega \xi (h_l - h_a) (r_l^2 \ln r_l - r_a^2 \ln r_a)}{2(1 - \mu_l) (r_a^2 - r_l^2) \ln (r_l / r_a)}$$

$$\chi_2 = \frac{r_a^2 r_l^2 (p_l - p_a)}{(r_l^2 - r_a^2)} + \frac{r_a^2 r_l^2 \gamma_\omega \xi (h_l - h_a)}{2(1 - \mu_l) (r_l^2 - r_a^2)}$$

$$\chi_3 = \frac{\gamma_\omega \xi (h_a - h_l)}{2(1 - \mu_l) \ln (r_l / r_a)}$$

$$\chi_4 = \frac{p_l r_l^2 - p_a r_a^2}{r_a^2 - r_l^2} + \frac{\gamma_\omega \xi (h_l - h_a) [(r_l^2 \ln r_l - r_a^2 \ln r_a) - (1 - 2\mu_l) (r_a^2 - r_l^2)]}{2(1 - \mu_l) (r_a^2 - r_l^2) \ln (r_l / r_a)}$$

3.3 围岩塑性区应力场

围岩塑性区中应力平衡方程为

$$\frac{d\sigma_\rho}{d\rho} + \frac{\sigma_\rho - \sigma_\theta}{\rho} + \frac{\gamma_\omega \xi (h_p - h_l)}{\rho \ln (r_p / r_l)} = 0 \quad (15)$$

由于在服役过程中, 海底隧道洞周的径向压应力较大, 环向压应力较小, 甚至转变为拉应力, 所以可将环向应力作为第一主应力。

D-P 准则为^[34]

$$f(I_1, \sqrt{J_2}) = \kappa I_1 + \sqrt{J_2} - \delta = 0 \quad (16)$$

式中

I_1 为应力第一不变量, $I_1 = \sigma_\rho + \sigma_\theta + \sigma_z$

J_2 为应力偏量第二不变量

$$J_2 = \frac{1}{6} [(\sigma_\rho - \sigma_\theta)^2 + (\sigma_\theta - \sigma_z)^2 + (\sigma_\rho - \sigma_z)^2]$$

κ 为与围岩摩擦角 φ 相关的常数

$$\kappa = \frac{\tan \varphi_p}{\sqrt{9 + 12 \tan^2 \varphi_p}}$$

δ 为与围岩黏聚力 c 相关的常数

$$\delta = \frac{3c_p}{\sqrt{9 + 12 \tan^2 \varphi_p}}$$

假定围岩塑性区形变时, 满足如下塑性应力-应

变关系^[35]

$$\left. \begin{aligned} de_\rho^p &= s_\rho d\Omega \\ de_\theta^p &= s_\theta d\Omega \\ de_z^p &= s_z d\Omega \end{aligned} \right\} \quad (17)$$

式中

$$s_\rho = \frac{1}{3} (2\sigma_\rho - \sigma_\theta - \sigma_z)$$

$$s_\theta = \frac{1}{3} (2\sigma_\theta - \sigma_\rho - \sigma_z)$$

$$s_z = \frac{1}{3} (2\sigma_z - \sigma_\rho - \sigma_\theta)$$

式中, de_ρ^p 为塑性应变径向偏量增量, de_θ^p 为塑性应变环向偏量增量, de_z^p 为塑性应变纵向偏量增量, s_ρ^p 为稳态应力径向偏量, s_θ^p 为稳态应力环向偏量, s_z^p 为稳态应力纵向偏量。

基于平面应变情况, 有 $de_z^p = 0$, 将其代入式 (17) 得

$$2\sigma_z = \sigma_\rho + \sigma_\theta \quad (18)$$

将式 (18) 代入 J_2 中, 联立式 (16), 得

$$\sigma_\rho - \sigma_\theta = -\frac{6\kappa}{1 - 3\kappa} \left(\sigma_\rho + \frac{\delta}{3\kappa} \right) \quad (19)$$

将式 (19) 代入式 (15), 得

$$\frac{d\sigma_\rho}{d\rho} - \frac{6\kappa}{1 - 3\kappa} \frac{\sigma_\rho + \Pi}{\rho} = 0 \quad (20)$$

式中

$$\Pi = \frac{\delta}{3\kappa} + \frac{1 + 3\kappa}{6\kappa} \frac{\gamma_\omega \xi (h_p - h_l)}{\ln (r_p / r_l)}$$

对式 (20) 积分得

$$\sigma_\rho = A r^{\frac{6\kappa}{1 - 3\kappa}} - \Pi \quad (21)$$

式中, A 为积分常量, $A = (p_l + \Pi) r_l^{-\frac{6\kappa}{1 - 3\kappa}}$ 。

根据边界条件 $(\sigma_\rho)_{r=r_l} = P_p = \gamma_\omega (h_p - h_0)$, 可得渗流效应下围岩塑性区应力场为

$$\left. \begin{aligned} \sigma_\rho^p &= p_l \left(\frac{r}{r_l} \right)^{-\frac{6\kappa}{1 - 3\kappa}} + \Pi \left[\left(\frac{r}{r_l} \right)^{-\frac{6\kappa}{1 - 3\kappa}} - 1 \right] \\ \sigma_\theta^p &= \frac{1 - 3\kappa}{1 + 3\kappa} \left[(p_l + \Pi) \left(\frac{r}{r_l} \right)^{-\frac{6\kappa}{1 - 3\kappa}} - \Pi \right] - \frac{2\delta}{1 + 3\kappa} \end{aligned} \right\} \quad (22)$$

3.4 围岩弹性区应力场

根据围岩弹、塑性区界面应力连续性条件, 得到渗流效应下围岩弹性区应力场为

$$\left. \begin{aligned} \sigma_\rho^e &= \gamma_\omega h_0(1-\xi) + \gamma_\omega \xi h_l + \frac{p_l \xi}{5.4(1-\mu_e)} \ln \frac{r}{r_0} + \frac{r_p^2}{r_p^2 - r_0^2} \frac{r_0^2 - r^2}{r^2} \\ &\left\{ \gamma_\omega h_0(1-\xi) + \gamma_\omega h_l \left[\xi - \left(\frac{r_p}{r_l} \right)^{-\frac{6\kappa}{1+3\kappa}} \right] + \Pi \left[1 - \left(\frac{r_p}{r_l} \right)^{-\frac{6\kappa}{1+3\kappa}} \right] + \frac{p_l \xi}{5.4(1-\mu_e)} \ln \frac{r}{r_0} \right\} \\ \sigma_\theta^e &= \gamma_\omega h_0(1-\xi) + \gamma_\omega \xi h_l + \frac{p_l \xi}{5.4(1-\mu_e)} \left(\ln \frac{r}{r_0} + 2\mu_e - 1 \right) - \\ &\frac{r_p^2}{r_p^2 - r_0^2} \frac{r_0^2 + r^2}{r^2} \left\{ \gamma_\omega h_0(1-\xi) + \gamma_\omega h_l \left[\xi - \left(\frac{r_p}{r_l} \right)^{-\frac{6\kappa}{1+3\kappa}} \right] + \Pi \left[1 - \left(\frac{r_p}{r_l} \right)^{-\frac{6\kappa}{1+3\kappa}} \right] + \frac{p_l \xi}{5.4(1-\mu_e)} \ln \frac{r_p}{r_0} \right\} \end{aligned} \right\} \quad (23)$$

3.5 围岩塑性区半径

根据应力连续性条件, 当 $r = r_p$ 时, 有 $(\sigma_\theta^e)_{r=r_p} = (\sigma_\theta^p)_{r=r_p}$, 联立式 (22) 和式 (23), 得

$$\begin{aligned} &\left(\frac{1-3\kappa}{1+3\kappa} - \frac{r_p^2 + r_0^2}{r_p^2 - r_0^2} \right) \left[(p_a + \Pi) \left(\frac{r_p}{r_a} \right)^{-\frac{6\kappa}{1+3\kappa}} - \Pi \right] - \\ &\frac{2\delta}{1+3\kappa} + \frac{2r_0^2}{r_p^2 - r_0^2} [p_0 + \gamma_\omega \xi (h_a - h_0)] = \\ &\frac{\gamma_\omega \xi (h_a - h_0)}{5.4(1-\mu_e)} \left(\ln \frac{r_p}{r_a} + 2\mu_e - 1 \right) - \\ &\frac{r_p^2 + r_0^2}{r_p^2 - r_0^2} \frac{\gamma_\omega \xi (h_a - h_0)}{5.4(1-\mu_e)} \ln \frac{r_p}{r_0} \end{aligned} \quad (24)$$

式 (24) 为围岩塑性区半径 r_p 的解答. 围岩塑性区半径 r_p 与地应力、内水压力 (或支护压力)、围岩强度参数、隧洞半径等有关.

将 r_p 代入式 (10), 推导出 h_l 和 h_p 的解析式, 进一步可后继得到 $(\sigma_\rho^l, \sigma_\theta^l)$, $(\sigma_\rho^p, \sigma_\theta^p)$ 和 $(\sigma_\rho^e, \sigma_\theta^e)$.

4 工程实例分析

当前隧道工程中多采用复合式衬砌结构, 二次衬砌施工前, 隧道围岩与初次衬砌已达到稳定状态, 本文在进行渗流分析时, 以作用在力学模型衬砌结构内边界的 p_a 和 h_a 替代了复合式衬砌结构中二次衬砌的堵水和支护作用, 可基于该模型研究渗流效应对围岩与初次衬砌应力场的影响.

4.1 工程背景

深圳妈湾跨海通道是濒海条件下, 穿港、深埋、特长的大型水下城市隧道工程^[5]. 该工程建设主要风险来自于复杂的地层条件, 尤其在濒海、深埋环境下, 海域段隧道周边岩层富水性强、水压高, 地下水渗流对隧道围岩及衬砌结构的影响不可忽

略, 渗流效应对该隧道稳定性的影响机理亟待研究.

4.2 讨论与分析

以深圳妈湾跨海通道为背景, 按照工程图纸各参数选取为: 隧道的内半径 $r_a = 4.7 \text{ m}$, 衬砌厚度为 0.3 m , 原始地应力 $P_0 = -10 \text{ MPa}$, 隧道内压力为 $P_a = 0$, 岩体有效孔隙水压力系数^[11,15] $\xi = 1.0$; 衬砌材料参数: 弹性模量 $E_l = 10 \text{ GPa}$, 泊松比 $\mu_l = 0.2$; 岩体材料参数: 弹性模量 $E_e = E_p = 1.0 \text{ GPa}$, 泊松比 $\mu_e = \mu_p = 0.35$, 黏聚力 $c_e = c_p = 1 \text{ MPa}$, 内摩擦角 $\varphi_e = \varphi_p = 40^\circ$.

图 3 结果表明, 随着 ρ 的增加: (1) 在衬砌结构中, 环向应力呈减小趋势, 由于衬砌结构刚度相较围岩更大, 导致围岩与衬砌结构界面出现应力跃变现象; (2) 在围岩塑性区, 环向应力呈增大趋势, 并在围岩弹、塑性区界面达到峰值; (3) 在围岩弹性区, 环向应力不断减小, 并最终趋于稳定; (4) 径向应力在围岩与衬砌结构中呈非线性增长. 本文理论解与有限元数值解结果基本一致.

图 4 给出了考虑渗流与不考虑渗流两种工况下

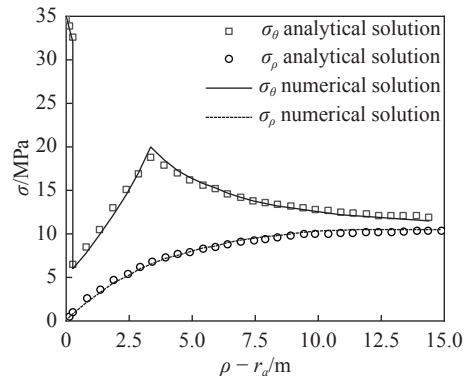


图 3 解析解与数值解对比

Fig. 3 Comparison of analytical solution and numerical solution

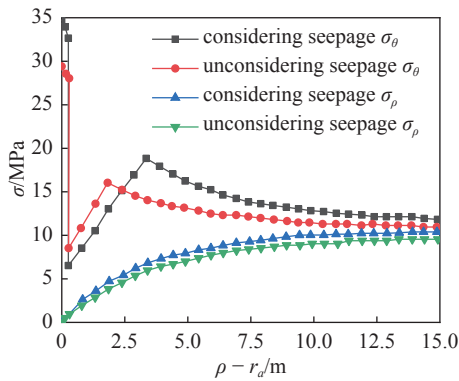


图 4 隧道应力分布

Fig. 4 Tunnel stress distribution

隧道应力 σ 与 ρ 的关系, 对于不考虑渗流的工况, 将内、外水压力差作为面力施加到模型各界面. 结果表明: 两种工况下随 ρ 的增加, 围岩与衬砌结构中应力变化趋势相同. 渗流效应对隧道围岩与衬砌结构中的环向应力增大效果明显, 若不考虑渗流效应将导致隧道应力计算结果误差较大.

图 5 给出了渗流效应下, 分别基于 M-C 准则和 D-P 准则计算得到的应力 σ 与 ρ 的关系, 结果表明: 本文应力计算结果与 M-C 准则计算结果基本吻合. 此外, 基于 D-P 准则计算得到的围岩塑性区半径大于 M-C 准则计算结果, 说明考虑渗流效应影响下, 通过 D-P 准则计算的结果更偏于安全, 实际工程中, 可以提高隧道设计合理性和施工安全性.

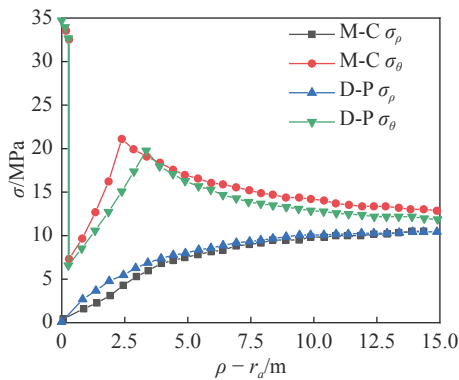


图 5 两种屈服准则下的隧道应力分布

Fig. 5 Tunnel stress distribution under two yield criteria

4.3 围岩塑性区半径影响因素

将考虑渗流与不考虑渗流两种工况下的计算结果进行对比. 其中, 不考虑渗流的工况, 将内、外水压力差作为面力施加到模型各界面.

4.3.1 海水深度 d_1 对围岩塑性区半径 r_p 的影响

图 6 给出了两种计算模型中 r_p/r_a 和 d_1 的关系,

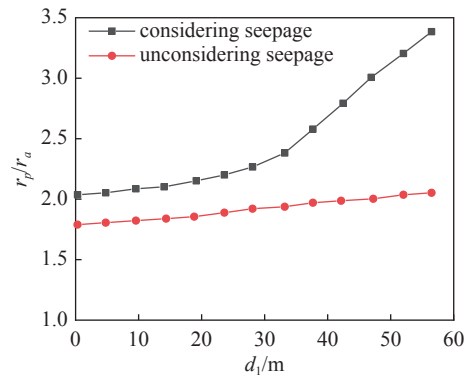


图 6 海水深度对塑性区半径影响

Fig. 6 The influence of seawater depth on the radius of the plastic zone

结果表明: 当隧道埋深不变时, 随着海水深度增加, 两种模型的围岩塑性区半径都呈增大趋势, 这与文献 [36] 中曲线趋势相同. 当海水深度较浅时, 隧道主要受上方覆盖含水岩层地下水的的作用, 围岩塑性区范围没有明显改变, d_1 对 r_p 的影响很小. 随着海水的加深, 作用于隧道周围的水头压力不断变大, 围岩塑性区范围有了明显增加, d_1 对 r_p 的影响显著.

4.3.2 内水水头 h_a 对围岩塑性区半径 r_p 的影响

图 7 给出了两种计算模型中 r_p/r_a 和 h_a 的关系, 结果表明: 随着内水水头的增加, 两种模型中围岩塑性区的发展都被有效限制, 初始阶段限制效果明显, 后续增加内水水头限制效果逐渐减弱. 对于不考虑渗流效应的工况, 将内水水头作为面力施加到模型中衬砌结构的内侧, h_a 对 r_a 的影响更为显著.

当内水水头增加到一定程度时, 围岩塑性区范围趋近于零, 表明内水水头对提升隧道稳定性有促进作用. 但值得注意的是, 这种作用并不是无限的, 当 h_a 增加超过 80 m 后, 对径向应力的影响大于环向应力, 导致围岩中主应力方向交换, 随之出现新的塑性区.

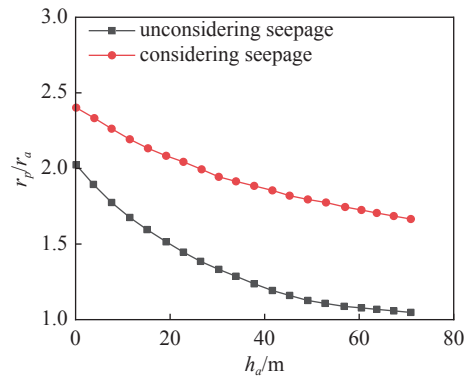


图 7 内水水头对塑性区半径影响

Fig. 7 The influence of internal water head on the radius of the plastic zone

5 结论

本文考虑渗流效应对海底隧道围岩与衬砌结构力学特性的影响,建立了由海水、岩体及衬砌结构组成的海底隧道力学模型,基于保角映射方法和 D-P 准则,得到了围岩渗流场及渗流效应影响下围岩与衬砌结构的弹塑性解析解,研究了渗流效应对隧道围岩与衬砌结构应力场的影响规律,分析了海水深度、内水水头对围岩塑性区半径的影响,并以深圳妈湾跨海通道工程为例,将解析解与有限元数值解进行了对比,得到以下结论。

(1) 由于围岩与衬砌结构的刚度相差较大,导致环向应力在围岩与衬砌结构界面出现跃变现象;围岩中的环向应力随半径增加呈先增大后减小的趋势,并在围岩弹、塑性区界面达到峰值。径向应力在围岩与衬砌结构中随半径增加呈非线性增长。

(2) 渗流效应对隧道围岩与衬砌结构中的环向应力增大效果显著,若不考虑渗流效应将导致隧道应力计算产生较大误差。

(3) 海水深度较浅时,受隧道上部覆盖层地下水作用,围岩塑性区范围无明显变化,随着海水加深,隧道承受水压不断加大,围岩塑性区范围显著增大。

(4) 内水水头的增加可以有效限制围岩塑性区的发展,初始阶段限制效果明显,后续增加内水水头限制效果逐渐减弱。如果内水水头增加超过 80 m,对径向应力的影响大于环向应力,导致围岩中主应力方向交换,出现新的塑性区。

参 考 文 献

- 张雨. 海底隧道水力流态特性研究及工程应用. [博士学位论文]. 北京: 北京交通大学, 2021 (Zhang Yu. Study on the hydraulic flow regime characteristics in subsea tunnels and its engineering application. [PhD Thesis]. Beijing: Beijing Jiaotong University, 2021 (in Chinese))
- He J. Research on deepening design and construction of cross-sea tunnel based on the principle of prefabricated building//IOP Conference Series: Earth and Environmental Science. OP Publishing, 2020, 598(1): 012016
- 刘强, 潘坚文, 金峰. 临海隧道渗流场解析解研究. 北京交通大学学报, 2019, 43(4): 18-28 (Liu Qiang, Pan Jinwen, Jin Feng. Study on analytic solution for seepage field of near-sea tunnel. *Journal of Beijing Jiaotong University*, 2019, 43(4): 18-28 (in Chinese))
- 陈小平, 辛丽敏, 孔祥岁等. 妈湾跨海通道工程隧道选线快速评价模型研究. 隧道建设, 2018, 38(10): 1630-1636 (Chen Xiaoping, Xin Limin, Kong Xiangsui, et al. Research on fast evaluation model for route selection of Mawan sea-crossing tunnel. *Tunnel Construction*, 2018, 38(10): 1630-1636 (in Chinese))
- 陈仁东. 妈湾跨海通道前海湾隧道工法方案比选. 地下空间与工程学报, 2017, 13(5): 1319-1328 (Chen Rendong. Comparison and selection for construction method of Qianhaiwan tunnel on Mawan cross passage. *Chinese Journal of Underground Space and Engineering*, 2017, 13(5): 1319-1328 (in Chinese))
- 袁大军, 吴俊, 沈翔等. 超高水压越江海长大盾构隧道工程安全. 中国公路学报, 2020, 33(12): 26-45 (Yuan Dajun, Wu Jun, Shen Xiang, et al. Engineering safety of cross-river or cross-sea long-distance large-diameter shield tunneling under superhigh water pressure. *China Journal of Highway and Transport*, 2020, 33(12): 26-45 (in Chinese))
- 赵建平, 李建武, 毕林等. 富水区隧道渗流场解析解及合理支护参数. 浙江大学学报(工学版), 2021, 55(11): 2142-2150 (Zhao Jianping, Li Jianwu, Bi Lin, et al. Analytical solution of seepage field and reasonable support parameters of tunnel in water rich area. *Journal of Zhejiang University (Engineering Science)*, 2021, 55(11): 2142-2150 (in Chinese))
- 郭玉峰, 王华宁, 蒋明镜. 水下浅埋双孔平行隧道渗流场的解析解研究. 岩体工程学报, 2021, 43(6): 1088-1096 (Guo Yufeng, Wang Huaning, Jiang Mingjing. Analytical solutions of seepage field for underwater shallow-buried parallel twin tunnels. *Chinese Journal of Geotechnical Engineering*, 2021, 43(6): 1088-1096 (in Chinese))
- Xue Y, Zhou B, Li S, et al. Deformation rule and mechanical characteristic analysis of subsea tunnel crossing weathered trough. *Tunnelling and Underground Space Technology*, 2021, 114: 103989
- Lee YK, Pietruszczak S. A new numerical procedure for elastoplastic analysis of a circular opening excavated in a strain-softening rock mass. *Tunnelling and Underground Space Technology*, 2008, 23(5): 588-599
- Li PF, Fang Q, Zhang DL. Analytical solutions of stresses and displacements for deep circular tunnels with liners in saturated ground. *Journal of Zhejiang University-Science A (Applied Physics & Engineering)*, 2014, 15(6): 395-404
- Li XF, Du SJ, Chen B. Unified analytical solution for deep circular tunnel with consideration of seepage pressure, grouting and lining. *Journal of Central South University*, 2017, 24(6): 1483-1493
- 邹金峰, 李帅帅, 张勇等. 考虑轴向力和渗透力时软化围岩隧道解析. 力学学报, 2014, 46(5): 747-755 (Zou Jinfeng, Li Shuaishuai, Zhang Yong, et al. Solution and analysis of circular tunnel for the strain-softening rock masses considering the axial in situ stress and seepage force. *Chinese Journal of Theoretical and Applied Mechanics*, 2014, 46(5): 747-755 (in Chinese))
- Ma Y, Lu A, Cai H, et al. Analytical solution for determining the plastic zones around two unequal circular tunnels. *Tunnelling and Underground Space Technology*, 2021, 120: 104267
- 彭立, 邹金峰, 彭建国等. 基于 Hoek-Brown 准则下的富水透水隧道非线性解析. 土木工程学报, 2011, 44(7): 149-156 (Peng L, Zou JF, Peng JG, et al. Nonlinear analytical solution for underwater tunnel using Hoek-Brown failure criterion. *China Civil Engineering Journal*, 2011, 44(7): 149-156 (in Chinese))
- Zhu C, Niu X, Liu X, et al. Comparative analysis on elastic-plastic analytical methods for tunnel surrounding rocks. *Tehnički vjesnik*, 2020, 27(2): 374-381
- 肖建清, 冯夏庭, 张腊春等. 均匀地应力场下圆形隧道静态弹塑性解析方法. 岩石力学与工程学报, 2013, 32(S2): 3466-3477 (Xiao JQ, Feng XT, Zhang LC, et al. Static elastoplastic analytical method of circular tunnel under uniform geostress field. *Chinese Journal of*

- Rock Mechanics and Engineering*, 2013, 32(S2): 3466-3477 (in Chinese))
- 18 Hu Y, Lei HY, Zheng G, et al. Assessing the deformation response of double-track overlapped tunnels using numerical simulation and field monitoring. *Journal of Rock Mechanics and Geotechnical Engineering*, 2022, 14(2): 436-447
- 19 Mu W, Li L, Chen D, et al. Long-term deformation and control structure of rheological tunnels based on numerical simulation and on-site monitoring. *Engineering Failure Analysis*, 2020, 118: 104928
- 20 何超, 周顺华, 狄宏规等. 饱和土—隧道动力响应的 2.5 维有限元—边界元耦合模型. *力学学报*, 2017, 49(1): 126-136 (He Chao, Zhou Shunhua, Di Honggui, et al. A 2.5D coupled FE-BE model for the dynamic interaction between tunnel and saturated soil. *Chinese Journal of Theoretical and Applied Mechanics*, 2017, 49(1): 126-136 (in Chinese))
- 21 何川, 齐春, 封坤等. 基于 D-P 准则的盾构隧道围岩与衬砌结构相互作用分析. *力学学报*, 2017, 49(1): 31-40 (He Chun, Qi Chun, Feng Kun, et al. Theoretical analysis of interaction between surrounding rocks and lining structure of shield tunnel based on Drucker-Prager yield criteria. *Chinese Journal of Theoretical and Applied Mechanics*, 2017, 49(1): 31-40 (in Chinese))
- 22 张顶立, 孙振宇, 侯艳娟. 隧道支护结构体系及其协同作用. *力学学报*, 2019, 51(2): 577-593 (Zhang Dingli, Sun Zhenyu, Hou Yanjuan. Tunnel support structure system and its synergistic effect. *Chinese Journal of Theoretical and Applied Mechanics*, 2019, 51(2): 577-593 (in Chinese))
- 23 Ma YF, Qin H, Zhang CM, et al. An elastic-plastic solution for a circular pressure tunnel with liner based on a new model. *International Journal of Earth Sciences and Engineering*, 2016, 9(6): 2354-2360
- 24 李岩松, 陈寿根. 寒区非圆形隧道冻胀力的解析解. *力学学报*, 2020, 52(1): 196-207 (Li Yansong, Chen Shougen. Analytical solution of frost heaving force in non-circular cold region tunnels. *Chinese Journal of Theoretical and Applied Mechanics*, 2020, 52(1): 196-207 (in Chinese))
- 25 Wang T, Zhou G, Wang JZ, et al. Stochastic analysis of uncertainty mechanical characteristics for surrounding rock and lining in cold region tunnels. *Cold Regions Science and Technology*, 2018, 145: 160-168
- 26 唐雄俊. 考虑围岩应变软化与剪胀效应的深埋隧道合理支护时机分析. *隧道建设*, 2021, 41(2): 1-9 (Tang Xiongjun. The reasonable tunnel support timing for the surrounding rock mass considering strain-softening and dilatancy behaviours. *Tunnel Construction*, 2021, 41(2): 1-9 (in Chinese))
- 27 Wang R, Liu XD, Bai JB, et al. An innovative elasto-plastic analysis for soft surrounding rock considering supporting opportunity based on Drucker-Prager Strength criterion. *Advances in Civil Engineering*, 2021, 2021(6): 1-9
- 28 Ying HW, Zhu CW, Shen HW. Semi-analytical solution for groundwater ingress into lined tunnel. *Tunnelling and Underground Space Technology*, 2018, 76: 43-47
- 29 Chen G, Ruan B, Zhao K, et al. Nonlinear response characteristics of undersea shield tunnel subjected to strong earthquake motions. *Journal of Earthquake Engineering*, 2020, 24(3): 351-380
- 30 张顶立. 隧道及地下工程的基本问题及其研究进展. *力学学报*, 2017, 49(1): 3-21 (Zhang Dingli. Essential issues and their research progress in tunnel and underground engineering. *Chinese Journal of Theoretical and Applied Mechanics*, 2017, 49(1): 3-21 (in Chinese))
- 31 Verruijt A. A complex variable solution for a deforming circular tunnel in an elastic half-plane. *International Journal for Numerical and Analytical Methods in Geomechanics*, 1997, 21(2): 77-89
- 32 Park KH, Owatsiriwong A, Lee JG. Analytical solution for steady-state groundwater inflow into a drained circular tunnel in a semi-infinite aquifer: a revisit. *Tunnelling and Underground Space Technology*, 2008, 23(2): 206-209
- 33 李宗利, 任青文, 王亚红. 考虑渗流场影响深埋圆形隧洞的弹塑性解. *岩石力学与工程学报*, 2004(8): 1291-1295 (Li Zongli, Ren Qingwen, Wang Yahong. Elasto-plastic analytical solution of deep-buried circle tunnel considering fluid flow field. *Chinese Journal of Rock Mechanics and Engineering*, 2004(8): 1291-1295 (in Chinese))
- 34 李建林. 卸荷岩体力学. 北京: 中国水利水电出版社, 2003 (Li Jianlin. Unloading Rock Mass Mechanics. Beijing: China Water Power Press, 2003 (in Chinese))
- 35 米海珍, 胡燕妮. 塑性力学. 北京: 清华大学出版社, 2014 (Mi Haizhen, Hu Yanni. Plasticity Theory. Beijing: Tsinghua University Press, 2014 (in Chinese))
- 36 吕晓聪, 许金余. 海底圆形隧道在渗流场影响下的弹塑性解. *工程力学*, 2009, 26(2): 216-221 (Lü Xiaocong, Xu Jinyu. Elastic-plastic solution for subsea circular tunnel under the influence of seepage field. *Engineering Mechanics*, 2009, 26(2): 216-221 (in Chinese))